JCTC Journal of Chemical Theory and Computation

Article

pubs.acs.org/JCTC

Multireference Second Order Perturbation Theory with a Simplified Treatment of Dynamical Correlation

Enhua Xu, Dongbo Zhao, and Shuhua Li*

School of Chemistry and Chemical Engineering, Key Laboratory of Mesoscopic Chemistry of Ministry of Education, Institute of Theoretical and Computational Chemistry, Nanjing University, Nanjing, 210093, P. R. China

ABSTRACT: A multireference second order perturbation theory based on a complete active space configuration interaction (CASCI) function or density matrix renormalized group (DMRG) function has been proposed. This method may be considered as an approximation to the CAS/A approach with the same reference, in which the dynamical correlation is simplified with blocked correlated second order perturbation theory based on the generalized valence bond (GVB) reference (GVB-BCPT2). This method, denoted as CASCI-BCPT2/GVB or DMRG-BCPT2/GVB, is size consistent and has a similar computational cost as the conventional second order perturbation theory (MP2). We have applied it to investigate a number of problems of chemical interest. These problems include bond-breaking potential energy surfaces in four molecules, the spectroscopic constants of six diatomic molecules, the reaction barrier for the automerization of cyclobutadiene, and the energy difference between the monocyclic and bicyclic forms of 2,6-pyridyne. Our test applications demonstrate that CASCI-BCPT2/GVB can provide comparable results with CASPT2 (second order perturbation theory based on the complete active space self-consistent-field wave function) for systems under study. Furthermore, the DMRG-BCPT2/GVB method is applicable to treat strongly correlated systems with large active spaces, which are beyond the capability of CASPT2.

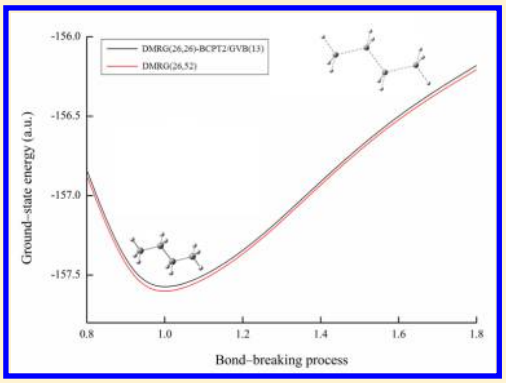

I. INTRODUCTION

The single-reference (SR) post-Hartree−Fock (post-HF) methods have achieved great success in describing electronic structures of closed-shell molecules near their equilibrium geometries. However, their accuracy deteriorates significantly for bond breaking processes and diradical (or polyradical) systems, in which the HF determinant is not a good zeroth-order wave function. For such cases, a multireference (MR) wave function, such as the complete active space self-consistent-field (CASSCF) wave function, is usually taken as the zeroth-order wave function. Since the static correlation within the active space is adequately described with a full configuration interaction (FCI) treatment, the CASSCF method is able to provide qualitatively correct descriptions for the multibond breaking processes. To further include the dynamic correlation energy, which results from the correlation between active electrons and inactive electrons, post-CASSCF correlation methods[1−21] should be developed. For instance, within the many-body perturbation theory framework, several schemes[1−8] have been proposed, which include the popular CASPT2 method (second order perturbation theory with the CASSCF reference function)[1−4] and the CAS/A method.[5] However, the traditional CASSCF-based correlation schemes are limited to systems with small active spaces. Several DMRG-based perturbation theories have been developed[22,23] to treat systems with large active spaces. However, their computational cost will increase quickly with the size of the active space. Thus, less expensive approaches, which are available for systems with large active spaces, are still needed.

In 2013, our group proposed a block correlated second order perturbation theory based on a generalized valence bond (GVB)[24] reference function (GVB-BCPT2),[25] whose computational cost is similar to that of the conventional single-reference second-order Møller−Plesset perturbation theory (MP2). The GVB-BCPT2 approach is demonstrated to have noticeably better performance than MP2 for systems with significant multireference character. However, it fails catastrophically in multibond breaking processes, due to the inappropriate treatment of interpair correlation.

In this work, we propose an alternative multireference second order perturbation theory based on a complete active space configuration interaction (CASCI) function or density matrix renormalized group (DMRG) function.[26−28] This method can be considered as an approximation to the CAS/A approach with the same reference, in which the dynamical correlation is simplified with the GVB-BCPT2 approach. This method, denoted as CASCI-BCPT2/GVB or DMRG-BCPT2/GVB, is size-consistent, and shares a similar computational cost as the conventional MP2 theory. The present method is applicable to much larger systems than the CAS/A method and can offer reasonably accurate descriptions for multibond breaking processes.

Received: May 26, 2015
Published: September 2, 2015

DOI: 10.1021/acs.jctc.5b00495
J. Chem. Theory Comput. 2015, 11, 4634−4643

The paper is arranged as follows: In section II, we will give a brief introduction to the CAS/A method and then describe the basic formulations and computational details of CASCI-BCPT2/GVB (or DMRG-BCPT2/GVB). In section III, the present method is applied to investigate bond-breaking potential energy surfaces in four systems, the spectroscopic constants in six diatomic molecules, the reaction barrier for the automerization of cyclobutadiene, and the energy difference between the monocyclic and bicyclic forms of 2,6-pyridyne. Finally, a brief summary will be given in section IV.

II. METHODOLOGY

A. A Brief Introduction to the CAS/A Method. Assume that all orbitals of a given system can be divided into three subgroups: closed-shell orbitals, virtual orbitals, and active orbitals. Thus, the multireference reference function of the CAS/A method can be formulated (in second-quantization form) as a direct product of the ground state wave function of each block:

$$|\Psi_0^{\mathrm{CAS/A}}\rangle = |M_0\rangle|N_0\rangle\ldots = |i_0\rangle|j_0\rangle\ldots|A_0\rangle|r_0\rangle|s_0\rangle\ldots \tag{1}$$

Here, i, j, ... (r, s, ...) represent occupied (or virtual) "single-spin-orbital" blocks; A is the active block which consists of all the active orbitals. In general, these blocks are denoted as M, N, ... The subscript 0 denotes the ground state. It is worth mentioning that $|A_0\rangle$ is a linear combination of many products of the creation operators of active orbitals (depending on the number of active electrons), $|i_0\rangle$ is just a creation operator of a closed-shell orbital, and $|r_0\rangle$ is a vacuum state. By construction, any "excited" configuration function (as shown below) can be formulated as

$$|\Psi_u^{\mathrm{CAS/A}}\rangle = \hat{T}_u^{\mathrm{CAS/A}}|\Psi_0^{\mathrm{CAS/A}}\rangle = \hat{A}^+_{M_\lambda}\hat{A}^-_{M_0}\hat{A}^+_{N_\eta}\hat{A}^-_{N_0}\cdots|\Psi_0^{\mathrm{CAS/A}}\rangle \tag{2}$$

Here, $\hat{T}_u^{\mathrm{CAS/A}}$ is a block-correlated operator that produces an "excited" configuration function from the reference function. $\hat{A}^+_{M_\lambda}$ is the creation operator that creates the λth excited state of block M (denoted as $|M_\lambda\rangle$) in the Fock space, while $\hat{A}^-_{M_0}$ represents the annihilation operator that destroys the ground state of block M. The subscript u is actually a compound index ($u = \{M_\lambda, N_\eta, \ldots\}$). By definition, all the excited configuration functions and the reference function are orthogonal to each other.

The zeroth-order Hamiltonian ($\hat{H}_0^{\mathrm{CAS/A}}$) of the CAS/A approach is defined as the summation of the individual Hamiltonians of all blocks:

$$\hat{H}_0^{\mathrm{CAS/A}} = \sum_i \varepsilon_i a_i^+ a_i^- + \sum_r \varepsilon_r a_r^+ a_r^- + \sum_{A_\lambda} E_{A_\lambda}\hat{A}^+_{A_\lambda}\hat{A}^-_{A_\lambda} \tag{3}$$

Here, the first two terms come from all "single-spin-orbital" blocks (closed-shell and virtual orbitals) and the last term from the active block, in which $\hat{A}^+_{A_\lambda}$ and $\hat{A}^-_{A_\lambda}$ are block-state creation and annihilation operators, respectively. With the CASSCF reference, we can define the following generalized Fock operator[5,29] for closed-shell and virtual orbitals:

$$\begin{aligned} A_{xy} = h_{xy} &+ \sum_m^{\mathrm{closed}} (\langle mx||my\rangle + \langle mx|my\rangle) \\ &+ \frac{1}{2}\sum_{P_u,P_v}^{\mathrm{act}} (\langle xp_u||yp_v\rangle + \langle xp_u|yp_v\rangle) \\ &\times (\langle A_0|P^+_{u\alpha}P^-_{v\alpha}|A_0\rangle + \langle A_0|P^+_{u\beta}P^-_{v\beta}|A_0\rangle) \end{aligned} \tag{4}$$

Here, $\hat{h}$ is the bare one-electron operator, (x,y) represents the closed-shell (or virtual) orbitals, and m and $P_{u(v)}$ are the spatial orbitals of the closed-shell and active space, respectively. Then, we diagonalize the Fock matrices (A_{xy}) separately for closed-shell and virtual orbital subspaces to obtain all the molecular orbitals and their orbital energies (ε_i for closed-shell orbitals and ε_r for virtual orbitals). While for the active block, its Hamiltonian is defined to include two-electron interactions within the active space:[5]

$$\begin{aligned} \hat{H}_A = &\sum_{w,x\in A} h_{wx}w^+x^- + \sum_{w,x,y,z\in A}\frac{1}{4}\langle wx||yz\rangle w^+x^+z^-y^- \\ &+ \sum_{w,x\in A} w^+x^- \sum_m^{\mathrm{closed}} (\langle wm||xm\rangle + \langle wm|xm\rangle) \end{aligned} \tag{5}$$

By diagonalizing the Hamiltonian ($\hat{H}_A$) within different Hilbert subspaces, we can get the block states (A_λ) and their block-state energies (E_{A_λ}) for the active block. It is worth mentioning that the CAS/A calculations based on GVB orbitals are also possible. In such cases, the active block is defined to include all open-shell orbitals and orbitals in all geminals.

Obviously, the reference function and all the excited configuration functions described above are constructed to be the eigenfunctions of $\hat{H}_0^{\mathrm{CAS/A}}$. Assume that the eigenvalues of $\hat{H}_0^{\mathrm{CAS/A}}$ are denoted as $E_0^{\mathrm{CAS/A}}$ and $\{E_u^{\mathrm{CAS/A}}\}$, the CAS/A energy up to the second order can be computed directly as below:

$$\begin{aligned} E_{\mathrm{CAS/A}} &= E_{\mathrm{CASCI}} \\ &+ \sum_{u\neq 0}\frac{|\langle\Psi_0^{\mathrm{CAS/A}}|(\hat{H} - \hat{H}_0^{\mathrm{CAS/A}})|\Psi_u^{\mathrm{CAS/A}}\rangle|^2}{E_0^{\mathrm{CAS/A}} - E_u^{\mathrm{CAS/A}}} \end{aligned} \tag{6}$$

Here, the reference function is usually taken as the complete active space configuration interaction (CASCI) function, which is a linear combination of all determinants from distributing active electrons into active orbitals. It is worth mentioning that the well-chosen reference function should describe the static correlation well. The second term in eq 6 is responsible for dynamical correlation. In principle, the static correlation should be modified in the presence of dynamical correlation. But this situation will not happen in the second order treatment of the CAS/A method. It has been demonstrated that CAS/A has a better performance than CASPT2 in dealing with the problem of intruder states.[5] However, since the number of the excited configuration functions increases exponentially with the size of the active space, the applications of the CAS/A method are limited to systems with small active spaces.

B. The CASCI-BCPT2/GVB Method. In order to extend the CAS/A method to systems with large active spaces, we have to introduce some approximations to simplify the calculation of the second term in eq 6. In fact, we can follow the ideas of the GVB-BCPT2 approach introduced in our previous work to achieve this goal. The basic idea is to approximate the CASCI reference and excited functions as the GVB reference and the

DOI: 10.1021/acs.jctc.5b00495
J. Chem. Theory Comput. 2015, 11, 4634−4643

corresponding excited functions, and simplify the zeroth-order Hamiltonian ($\hat{H}_0^{\mathrm{CAS/A}}$) as the zeroth-order Hamiltonian ($\hat{H}_0^{\mathrm{GVB}}$) in computing the second term in eq 6. The resulting method is named CASCI-BCPT2/GVB for convenience. First, the GVB reference can be formulated as a direct product of the ground state wave function of each block as below:

$$|\Psi_0^{\mathrm{GVB}}\rangle = |M_0\rangle|N_0\rangle\ldots = |i_0\rangle|j_0\rangle\ldots|P_0\rangle|Q_0\rangle\ldots|r_0\rangle|s_0\rangle\ldots \tag{7}$$

Here, P (Q) represents a geminal block, which contains two electrons and two orbitals. The ground state of the geminal block can be expressed as below:

$$|P_0\rangle = (c_{P_{0,1}} p_{1\alpha}^+ p_{1\beta}^+ + c_{P_{0,2}} p_{2\alpha}^+ p_{2\beta}^+)|\mathrm{vac}\rangle \tag{8}$$

in which p_1 and p_2 are the natural orbitals and $c_{P_{0,1}}$ and $c_{P_{0,2}}$ are the pair coefficients. Since there are only two orbitals and two electrons within each geminal, the number of the excited states within the Fock space for each geminal is 15.[25] The block correlated operators $\{\hat{T}_u^{\mathrm{GVB}}\}$, which can produce the corresponding excited configuration functions $\{|\Psi_u^{\mathrm{GVB}}\rangle\}$ by acting on the GVB reference function, are listed in Appendix A. Since the role of the second term in eq 6 is to add semiexternal and external dynamical correlation involving active blocks and closed-shell or virtual orbitals, the block-correlated operators involving active blocks (geminals or open-shell spin orbitals) only should be excluded.

Second, the zeroth-order Hamiltonian ($\hat{H}_0^{\mathrm{GVB}}$) in CASCI-BCPT2/GVB may be considered as an approximation to $\hat{H}_0^{\mathrm{CAS/A}}$ in CAS/A:

$$\hat{H}_0^{\mathrm{GVB}} = \sum_i \varepsilon_i a_i^+ a_i^- + \sum_r \varepsilon_r a_r^+ a_r^- + \sum_P \sum_{\lambda\in P} E_{P_\lambda} \hat{A}_{P_\lambda}^+ \hat{A}_{P_\lambda}^- \tag{9}$$

Here, the first two terms come from all "single-spin-orbital" blocks, which may include some open-shell orbitals, while the last term comes from all the geminal blocks. Now we will discuss how to obtain orbitals and block states for CASCI-BCPT2/GVB calculations. First, a standard GVB calculation is done to get open-shell orbitals and geminals. Then, we construct a generalized Fock operator (F_{xy})[25,29] for each type of orbital (closed-shell, open-shell, and virtual), as done in our previous GVB-BCPT2 approach. However, in this work, for open-shell orbitals the corresponding Fock operator is defined as

$$G_{kl} = h_{kl} + \sum_m^{\mathrm{closed}} (\langle mk||ml\rangle + \langle mk|ml\rangle) + \sum_n^{\mathrm{open}} \langle nk||nl\rangle + \sum_P^{\mathrm{gem}} \sum_{v=1,2} (c_{P_{0,v}})^2 (\langle kp_v||lp_v\rangle + \langle kp_v|lp_v\rangle) \tag{10}$$

Here, (k, l) represents the open-shell orbitals and P_v, m, and n are the natural orbitals of different geminals, closed-shell spatial orbitals, and open-shell spatial orbitals, respectively. In the last step, we diagonalize the Fock matrices separately for closed-shell (F_{xy}), open-shell (G_{kl}), and virtual subspaces (F_{xy}), to obtain all the molecular orbitals and their orbital energies.

For a geminal block P, its individual Hamiltonian is defined as

$$\hat{H}_P = \sum_{w,x\in P} h_{wx} w^+ x^- + \sum_{w,x,y,z\in P} \frac{1}{4}\langle wx||yz\rangle w^+ x^+ z^- y^- + \sum_{w,x\in P} w^+ x^- \left(\sum_{Q\neq P} \sum_{l\in Q} c_{Q_{0,l}}^2 \times \langle wl||xl\rangle + \sum_m^{\mathrm{closed}} (\langle wm||xm\rangle + \langle wm|xm\rangle) + \frac{1}{2}\sum_n^{\mathrm{open}} (\langle wn||xn\rangle + \langle wn|xn\rangle) \right) \tag{11}$$

By diagonalizing the Hamiltonian described above within different Hilbert subspaces, we can get the block states (P_λ) and their block-state energies (E_{P_λ}) of each geminal block.

Since the GVB reference function Ψ_0^{GVB} and its excited configuration functions $\{|\Psi_u^{\mathrm{GVB}}\rangle\}$ are constructed to be the eigenfunctions of $\hat{H}_0^{\mathrm{GVB}}$, the corresponding eigenvalues can be formulated as below:

$$E_0^{\mathrm{GVB}} = \sum_i \varepsilon_i + \sum_P E_{P_0} \tag{12}$$

$$E_u^{\mathrm{GVB}} = E_0^{\mathrm{GVB}} + \sum_{u=\{M_\lambda, N_\eta,\ldots\}} (E_{M_\lambda} - E_{M_0} + E_{N_\eta} - E_{N_0} + \ldots) \tag{13}$$

Thus, the CASCI-BCPT2/GVB energy can be expressed as

$$E_{\mathrm{CASCI-BCPT2/GVB}} = E_{\mathrm{CASCI}} + \sum_{u\neq 0} \frac{|\langle\Psi_0^{\mathrm{GVB}}|(\hat{H} - \hat{H}_0^{\mathrm{GVB}})|\Psi_u^{\mathrm{GVB}}\rangle|^2}{E_0^{\mathrm{GVB}} - E_u^{\mathrm{GVB}}} \tag{14}$$

The computation of the Hamiltonian matrix elements involved in eq 14 is straightforward, as shown in the Appendix B. The computational cost of the CASCI-BCPT2/GVB method is very similar to that of the conventional MP2 theory. Like the GVB-BCPT2 approach, the present CASCI-BCPT2/GVB method is also expected to be size consistent. From the discussions above, one may consider the CASCI-BCPT2/GVB method as an approximation to the CAS/A method. Due to the much lesser computational cost, the CASCI-BCPT2/GVB method is expected to be applicable to systems with large active spaces. Especially, for systems with relatively large active spaces, the DMRG wave function may take the role of the CASCI reference function. For such systems, one may perform DMRG-BCPT2/GVB calculations instead.

It should be mentioned that, for systems involving breaking of two or more covalent bonds, the ground-state and excited-state energies of some geminals may become nearly degenerate ($E_{P_0} \approx E_{P_\lambda}$), and thus the GVB-BCPT2 energy may diverge (due to small denominators). However, CASCI-BCPT2/GVB does not have this difficulty. A main reason is the absence of pure active excitations among different geminals in eq 14. In addition, in a reasonable GVB wave function, all the valence electrons should be described with geminals or open-shell orbitals. Hence, the energies of the orbitals in active blocks (geminals and open-shell blocks) are lower than those of the virtual orbitals but higher than those of the closed-shell orbitals. Since each excited configuration function in eq 14 corresponds

DOI: 10.1021/acs.jctc.5b00495
J. Chem. Theory Comput. 2015, 11, 4634−4643

Table 1. Ground-State Energies Obtained Using Various Theoretical Methods with the Cartesian cc-pVDZ Basis Set for Simultaneous Bond Dissociation in H_2O[a]

R (R_e)	GVB	GVB-BCPT2	CASCI-BCPT2/GVB	CAS/A[b]	CASSCF	CASPT2	DMRG
1.0	178.60	10.17	10.10	15.49 (16.08)	169.19	13.31	−76.24549
1.5	164.31	10.99	10.71	13.89 (13.96)	156.31	11.53	−76.07575
2.0	147.30	10.50	14.24	15.35 (15.36)	137.91	8.45	−75.95484
2.5	145.89	−34.45	14.07	15.46 (15.44)	129.56	8.08	−75.92100
3.0	146.55	−309.62	13.26	14.54 (14.51)	126.88	7.42	−75.91411
5.0	147.80	−5.31E5	14.05	15.26 (15.23)	127.12	8.27	−75.91326
MAE	178.60	5.31E5	14.24	15.49 (16.08)	169.19	13.31	
NPE	32.71	5.31E5	4.14	1.60 (2.12)	42.31	5.89	

[a]The bond angle is fixed at ∠HOH = 110.6°, and R_e = 0.97551 Å. DMRG(2000) energies (hartree) are taken as the reference data. The values for GVB, GVB-BCPT2, CASCI-BCPT2/GVB, CAS/A, CASSCF, and CASPT2 are the deviations with respect to the reference data in millihartree (mH). [b]The CAS/A values based on the CASSCF orbitals are included in parentheses.

Table 2. Ground-State Energies Obtained Using Various Theoretical Methods with the cc-pVDZ and cc-pVTZ Basis Sets for the Triple Bond Breaking Process in N_2[a]

			cc-pVDZ			
R (bohr)	GVB	CASCI-BCPT2/GVB	CAS/A[b]	CASSCF	CASPT2	DMRG
2.118	253.94	23.94	34.20 (33.98)	191.60	22.57	−109.28287
2.4	263.60	24.19	34.31 (33.58)	195.26	22.91	−109.24271
2.7	268.40	24.00	33.62 (33.02)	198.63	22.25	−109.16447
3.0	267.49	24.42	32.83 (32.77)	200.79	20.21	−109.09015
3.6	264.31	26.36	33.41 (33.74)	197.64	14.58	−108.99805
4.5	278.63	25.90	33.68 (33.54)	187.39	13.53	−108.96551
MAE	278.63	26.36	34.31 (33.98)	200.79	22.91	
NPE	24.69	2.42	1.48 (1.21)	13.40	9.38	
			cc-pVTZ			
R (bohr)	GVB	CASCI-BCPT2/GVB	CAS/A[b]	CASSCF	CASPT2	DMRG
2.118	319.15	29.85	40.47 (39.56)	257.50	24.71	−109.37691
2.4	326.13	29.60	40.04 (38.54)	258.60	24.40	−109.32994
2.7	329.29	28.22	38.52 (37.36)	260.15	22.76	−109.24839
3.0	327.38	27.21	36.97 (36.76)	261.02	19.72	−109.17231
3.6	320.71	26.28	36.61 (37.20)	254.73	11.82	−109.07482
4.5	330.67	23.62	36.53 (36.26)	240.68	10.23	−109.03653
MAE	330.67	29.85	40.04 (39.56)	261.02	24.71	
NPE	11.52	6.23	3.94 (3.30)	20.34	14.48	

[a]DMRG(2000) energies (hartree) are taken as the reference data at both basis sets. The values for GVB, CASCI-BCPT2/GVB, CAS/A, CASSCF, and CASPT2 are the deviations with respect to the reference data in mH. [b]The CAS/A values based on the CASSCF orbitals are included in parentheses.

to the excitation of electrons from lower-energy blocks to higher-energy blocks, the denominator ($E_0^{GVB} - E_u^{GVB}$) in eq 14 will not come close to zero. Hence, with a reasonably chosen GVB reference, the CASCI-BCPT2/GVB method can avoid the divergence problem of the original GVB-BCPT2 method. Our numerical results in the next section also support this analysis.

C. Implementation Details. In the present implementation, the one-electron and two-electron integrals are obtained by running the GAMESS[30] program. Then, our own program is used to determine the molecular orbitals with orbital energies and the block states with block−state energies for all geminals (for GVB-BCPT2 and CASCI-BCPT2/GVB) or a general active block (for CAS/A). The CASCI-BCPT2/GVB method can be easily implemented by slightly modifying the original GVB-BCPT2 program. If the active space is small, our own CASCI program is performed. Otherwise, the BLOCK program[31−34] from Chan's group is performed for DMRG calculations. The total energies within the CAS/A and CASCI-BCPT2/GVB (or DMRG-BCPT2/GVB) frameworks are obtained via eq 6 and eq 14, respectively.

III. RESULTS AND DISCUSSIONS

In this section, we will apply the CASCI-BCPT2/GVB (or DMRG-BCPT2/GVB) method to a number of systems to demonstrate its accuracy and applicability. For these systems, we will also compare the results from our methods with those from other theoretical methods or the experimental data. To obtain results from other theoretical methods, we have performed CASPT2[35−37] calculations with the MOLRPO program,[38] and CCSD (coupled cluster singles and doubles)[39−42] and CCSD(T) (coupled cluster singles, doubles and perturbative triples)[43] calculations with the GAMESS program. For convenience, (n_e, n_o) is used to represent the active space with n_e active electrons in n_o active orbitals employed in CASSCF, CASCI, CAS/A, and DMRG calculations. For a given system, the orbitals employed in GVB-BCPT2, CASCI-BCPT2/GVB (or DMRG-BCPT2/GVB), and CAS/A calculations are derived from a standard GVB calculation. In some

DOI: 10.1021/acs.jctc.5b00495
J. Chem. Theory Comput. 2015, 11, 4634−4643

Table 3. Ground-State Energies Obtained Using Various Methods at the Cartesian 6-31G** Basis Set for a Methane Molecule[a]

R (Å)	GVB	CASCI-BCPT2/GVB	CAS/A[b]	CASSCF	CASPT2	DMRG
1.0	140.22	27.22	26.75 (26.00)	119.05	15.93	−40.37160
1.2	125.39	22.21	22.03 (21.06)	102.78	13.84	−40.36825
1.5	110.64	15.82	15.76 (14.34)	81.57	10.05	−40.17464
1.8	113.16	14.02	12.89 (11.33)	69.39	7.42	−39.97766
2.1	141.62	17.94	13.45 (11.32)	65.97	5.95	−39.85028
2.4	190.67	23.33	14.43 (11.99)	65.11	5.41	−39.78936
2.7	239.35	25.28	14.19 (12.36)	63.72	5.48	−39.76485
3.0	274.01	25.62	13.62 (12.44)	62.66	5.74	−39.75562
3.3	292.72	26.14	13.29 (12.46)	62.10	5.92	−39.75212
MAE	303.92	27.22	26.75 (26.00)	119.05	15.93	
NPE	193.28	13.20	13.87 (14.68)	58.48	10.52	

[a]The bond angles are fixed when all the bond distances are stretched from 1.0 to 3.3 Å. The DMRG(2000) energies (hartree) are taken as the reference data. The values for GVB, CASCI-BCPT2/GVB, CAS/A, CASSCF, and CASPT2 are the deviations with respect to the reference data in mH. [b]The CAS/A values based on the CASSCF orbitals are included in parentheses.

cases, we also performed CAS/A calculations based on the CASSCF orbitals. A comparison of the CAS/A results based on GVB and CASSCF orbitals may be used to judge whether the GVB orbitals are good approximations to CASSCF orbitals.

A. Bond Breaking Potential Energy Surfaces. In this subsection, we will investigate the performance of the CASCI-BCPT2/GVB (or DMRG-BCPT2/GVB) method on multi-bond dissociation processes in four typical systems. The first example is the simultaneous dissociation of two O−H bonds in H_2O. In our calculations, the H−O−H angle is fixed at 110.6°, and the O−H bond is set to be at the equilibrium distance (R_e = 0.97551 Å). We have calculated the ground-state energies with several methods at a series of O−H bond distances at Cartesian cc-pVDZ basis set. The orbitals from GVB(2) calculations are employed in GVB-BCPT2, CASCI-BCPT2/GVB, and CAS/A calculations, and the CASSCF(4,4) wave function is employed as the reference for CASPT2 calculations. The maximum absolute errors (MAEs) and the nonparallelity errors (NPEs) of GVB(2), GVB(2)-BCPT2, CASCI-BCPT2/GVB(2), CASSCF(4,4), CAS/A(4,4), and CASPT2(4,4) with respect to the DMRG energies are listed in Table 1. Here, DMRG results obtained with 2000 states [DMRG(2000)] are correct to four decimal places to the full CI results. It can be seen from Table 1 that GVB(2)-BCPT2 breaks down when the O−H distance is larger than 2.5 R_e. The NPE value of GVB(2)-BCPT2 is as large as 5.3E5 milihartree (mH). However, one can notice that the CAS/A values based on GVB and CASSCF orbitals are very close to each other, with the NPE values of only 1.60 and 2.12 mH, respectively. In addition, the largest deviation between CASSCF and CASCI (based on GVB orbitals) energies is only 1.03 mH. These results suggest that GVB orbitals are quite good approximations to CASSCF orbitals. The CASCI-BCPT2/GVB(2) approach is a good approximation to the CAS/A method, with the NPE value of 4.14 mH. The CASPT2(4,4) method has a slightly larger NPE value (5.89 mH).

The second example is the triple bond breaking process in N_2. Two Cartesian basis sets (cc-pVDZ and cc-pVTZ) are employed. With orbitals from GVB(3) calculations, the (6,6) active space is used in CASCI and CAS/A calculations. The core orbitals are frozen in correlation calculations. The MAEs and NPEs of several approaches at various N−N bond lengths with respect to the DMRG(2000) energies are listed in Table 2. The CASCI-BCPT2/GVB(3) approach is able to provide satisfactory descriptions, with the NPE values being only 2.4 and 6.2 mH at cc-pVDZ and cc-pVTZ basis sets, respectively. The performance of the CAS/A method (with both GVB and CASSCF orbitals) is still the best, with the NPE values of less than 1.5 and 4.0 mH at cc-pVDZ and cc-pVTZ basis sets, respectively. The CAS/A results based on GVB orbitals are excellent approximations to those based on CASSCF orbitals. The CASCI-BCPT2/GVB(3) approach has a smaller NPE value than the CASPT2(6,6) method at both basis sets.

The third example is the simultaneous bond dissociation of four single bonds in methane. The Cartesian 6-31G** basis set is employed. The potential energy surface of this molecule at a series of C−H bond distances from 1.0 to 3.3 Å (all the bond angels are fixed) is investigated with several methods. With orbitals from GVB(4) calculations, the (8,8) active space is used in CASCI and CAS/A calculations. The CASSCF(8,8) wave function is employed as the reference for CASPT2 method. The MAEs and NPEs of several methods at various C−H bond distances with respect to the DMRG(2000) energies are listed in Table 3. The CASCI-BCPT2/GVB(4) approach is able to provide reasonable descriptions, with the NPE value of 13.2 mH. The CASPT2(8,8) method has the best performance, with the NPE value of 10.5 mH. The CAS/A results based on GVB and CASSCF orbitals are also in good agreement with each other, and the performance of the CAS/A method is similar to that of the CASCI-BCPT2/GVB(4) method.

The last example is the simultaneous bond dissociation of 13 single bonds in an *n*-butane molecule. The equilibrium geometry of this molecule is optimized with the B3LYP method at the 6-31G basis set. Then, the potential energy surface of this molecule with all the bond distances simultaneously stretched from their 0.8 R_e to 1.8 R_e (all the bond angels are fixed at their equilibrium values) is investigated with several methods. The equilibrium geometry and its distorted structure with all bond distances being 1.8 R_e are shown in Figure 1. The ground-state energies of this system at various bond distances at the 6-31G basis set are calculated from DMRG calculations with 2000 states, in which 26 electrons are distributed into 52 orbitals (four core orbitals are frozen in correlation calculations and the remaining occupied and virtual orbitals are localized separately). To describe the dissociation of all C−C and C−H bonds, we have to perform GVB(13) calculations to get the orbitals and geminals. It should be mentioned that at bond distances beyond 1.8 R_e, we could not obtain converged GVB energies for this molecule.

DOI: 10.1021/acs.jctc.5b00495
J. Chem. Theory Comput. 2015, 11, 4634−4643

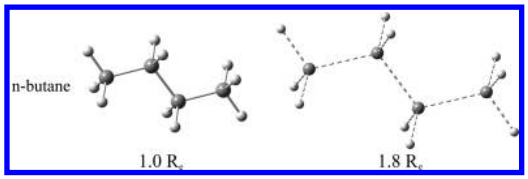

Figure 1. Equilibrium geometry of *n*-butane (optimized at the B3LYP/6-31G level) and its distorted structure. In the distorted structure, all the bond distances are stretched from their equilibrium distances to 1.8 R_e, while all the bond angels are fixed during this process.

Since CASSCF, CASPT2, and CAS/A calculations are not feasible for this system, only DMRG(26,26), GVB(13)-BCPT2, and DMRG(26,26)-BCPT2/GVB(13) results are listed in Table 4. Here, 1000 states are used in DMRG(26,26) calculations, in which 13 pairs of electrons are distributed into 26 geminal orbitals from GVB(13) calculations. One can see that during the bond breaking process of this molecule, GVB(13)-BCPT2 is not able to provide satisfactory descriptions, with the NPE value being 102.8 mH. However, the DMRG(26,26)-BCPT2/GVB(13) approach can provide reasonably accurate results, with the NPE value of 16.3 mH. The performance of DMRG(26,26) is much worse than that of DMRG(26,26)-BCPT2/GVB(13). This result indicates that DMRG-BCPT2/GVB is effective in evaluating the dynamical correlation. To conclude from this subsection, one can see that the CASCI-BCPT2/GVB method can provide reasonably accurate descriptions for dissociation of multiple bonds and simultaneous dissociation of many single bonds.

B. Equilibrium Distances and Spectroscopic Constants in Diatomic Molecules. For five diatomic molecules including C_2 ($^1\Sigma_g^+$),[44] CN ($^2\Sigma^+$),[44] ScO ($^2\Sigma^+$),[45] TiN ($^2\Sigma^+$),[46,47] and VN ($^3\Delta$),[48] we have calculated their ground-state equilibrium distances (R_e), vibration frequencies (ω_e), and anharmonicity constants ($\omega_e x_e$) with GVB-BCPT2, CASCI-BCPT2/GVB, and CASPT2 methods. The Cartesian cc-pVTZ basis set is employed, and all electrons are correlated in calculations. In the GVB reference, there are four geminals for C_2, and three geminals for the other four molecules. The values obtained by fitting the potential energy profiles (around the equilibrium distance) as a sixth degree polynomial potential are listed in Table 5. One can see that the overall performance of CASCI-BCPT2/GVB is noticeably better than GVB-BCPT2, especially for CN. The deviations of GVB-BCPT2 vibration frequencies and anharmonicity constants (relative to the experimental data) in CN reach up to 196 and 110.6 cm^{-1}, respectively, while the deviations from CASCI-BCPT2/GVB are only 1 and 0.6 cm^{-1}, respectively. Among the three methods, the CASPT2 method shows the best overall performance. Nevertheless, without using the IP-EA (ionization potential-electron affinity) shift, the CASPT2 method implemented in MOLPRO cannot give converged results for TiN and VN molecules.

The CASCI-BCPT2/GVB method is also employed to study the spectroscopic properties for the ground state of Cr_2 ($^1\Sigma_g^+$).[49−53] For this system, six geminals are employed to describe the hextuple bonds in Cr_2. The Cartesian cc-pVTZ basis set is employed, and all electrons are correlated in our

Table 5. Equilibrium Distances (R_e), Vibration Frequencies (ω_e) and Anharmonicity Constants ($\omega_e x_e$) Calculated with Different Methods for the Ground State of Several Diatomic Molecules[a]

	GVB-BCPT2	CASCI-BCPT2/GVB	CASPT2	exptl.[b]
		R_e (Å)		
C_2	1.257	1.247	1.245	1.243
CN	1.172	1.175	1.178	1.172
ScO	1.663	1.659	1.664	1.668
TiN	1.572	1.58	1.584	1.583
VN	1.555	1.556	1.564	1.574
max	0.019	0.018	0.010	
mean	0.007	0.005	0.003	
		ω_e (cm^{-1})		
C_2	1853	1859	1871	1855
CN	2265	2070	2038	2069
ScO	1023	1029	997	965
TiN	1107	1093	1048	1050
VN	1055	1081	1031	1033
max	196	64	32	
mean	48	23	12	
		$\omega_e x_e$ (cm^{-1})		
C_2	9.5	14	13	13.3
CN	−97.5	12.5	12.9	13.1
ScO	9	7.3	4.6	4.2
TiN	8.5	3	5.2	5.1
VN	7.4	5.5	6.9	6.7
max	110.6	3.1	0.4	
mean	17.6	1.1	0.2	

[a]The cc-pVTZ basis set is employed. There are four geminals for C_2 and three geminals for CN, ScO, TiN, and VN. All the electrons are correlated in correlation calculations. [b]Ref 44 for C_2 and CN, ref 45 for ScO, refs 46 and 47 for TiN, and ref 48 for VN.

Table 4. Ground-State Energies Obtained Using Various Methods at the 6-31G Basis Set for a *n*-Butane Molecule[a]

R (R_e)	GVB(13)	DMRG(26,26)	GVB(13)-BCPT2	DMRG(26,26)-BCPT2/GVB(13)	DMRG(26,52)
0.8	234.12	164.14	41.37	35.77	−156.87679
0.9	237.68	159.02	36.22	32.01	−157.50490
1.0	239.26	149.75	30.80	27.78	−157.67025
1.2	246.53	129.56	24.06	21.34	−157.40186
1.4	271.97	118.59	30.15	19.43	−156.92275
1.6	327.91	119.75	59.89	21.34	−156.50091
1.8	427.45	129.37	126.88	26.44	−156.20666
MAE	427.45	164.14	126.88	35.77	
NPE	188.19	45.55	102.82	16.34	

[a]The bond angles are fixed when all the bond distances are stretched from 0.8 R_e to 1.8 R_e. The DMRG(26,52) energies (hartree) are taken as the reference data. The values for GVB(13), DMRG(26,26), GVB(13)-BCPT2, and DMRG(26,26)-BCPT2/GVB(13) are the deviations with respect to the reference data in mH.

DOI: 10.1021/acs.jctc.5b00495
J. Chem. Theory Comput. 2015, 11, 4634−4643

calculations. Unfortunately, GVB(6)-BCPT2 cannot provide the spectroscopic data of this molecule, since the GVB(6)-BCPT2 energy diverges. This fact reflects that the intergeminal correlation is very strong in Cr_2 even around its equilibrium geometry. The CASCI-BCPT2/GVB(6) approach, in which the intergeminal correlation is described with CASCI(12,12), is able to provide acceptable equilibrium distance R_e (1.605 Å) and vibration frequency ω_e (624 cm^{-1}), and dissociation energy D_e (1.56 eV), as shown in Table 6. The performance of

Table 6. Calculated and Experimental Spectroscopic Data for the Ground State of Cr_2

methods	R_e (Å)	ω_e (cm^{-1})	D_e (eV)
CASCI-BCPT2/GVB(6)[a]	1.605	624	1.56
CASPT2(12,12)[b]	1.695	534	1.66
DMRG-CASPT2(12,28)[c]	1.682	471	1.56
MR-AQCC(12,12)[d]	1.685	459	1.36
exptl.	1.679[e]	481[f]	1.45−1.56[g]

[a]Cartesian cc-pVTZ basis set is employed and all electrons are correlated. [b]Ref 54. [c]Ref 55. [d]Ref 56. [e]Ref 49. [f]Ref 50. [g]Refs 51−53.

CASPT2(12,12)[54] is somewhat better than that of CASCI-BCPT2/GVB(6). There are two directions for improving the descriptions. First, one may employ larger active spaces (by adding more virtual orbitals into the active space). As shown previously, DMRG-CASPT2(12,28)[55] calculations can offer better results than CASPT2(12,12) calculations (see Table 6). Second, the active space maintains the original size, but the dynamical correlation is described with a more accurate method. The MR-AQCC(12,12) (multireference average-quadratic coupled cluster)[56] method is also demonstrated to be more accurate than CASPT2(12,12). Along this direction, higher order perturbation corrections within the CASCI-BCPT2/GVB framework may be considered in the future.

C. The Barrier Height of the Automerization Reaction of Cyclobutadiene. We have applied the CASCI-BCPT2/GVB method to calculate the barrier height of the automerization reaction of cyclobutadiene. The geometries of the reactant and the transition state optimized with the MR-AQCC method[57] at the cc-pVTZ basis set are displayed in Figure 2. With orbitals from GVB(2) calculations, the (4,4) active space, which contains four π electrons in four π orbitals, is used in CASCI and CAS/A calculations. With zero-point energy (ZPE) corrections (−2.5 kcal/mol at the MR-AQCC/cc-pVDZ level), the calculated energy barriers obtained with different methods are listed in Table 7. The core orbitals are frozen in all electron correlation calculations. It can be seen from Table 7 that GVB(2)-BCPT2 predicts a much higher barrier height (18.6 kcal/mol) than the experimental estimate (1.6−10.0 kcal/mol),[58] while CASCI-BCPT2/GVB(2) predicts a barrier of 11.8 kcal/mol, being close to the CAS/A barrier with GVB orbitals (10.3 kcal/mol). The CAS-BCCC4[59] and MR-AQCC methods provide similar barrier heights. If we consider their values as the reference data, the deviations of CASCI-BCPT2/GVB and CASPT2 barriers are quite similar. Surprisingly, the CAS/A barrier based on the CASSCF orbitals (6.92 kcal/mol) is much closer to the reference data than that with the GVB orbitals (10.33 kcal/mol). This result indicates that GVB orbitals are not good mimics of CASSCF orbitals. By analyzing the components of GVB orbitals, we find that for this system GVB orbitals in the transition state are noticeably delocalized compared to those in the reactant. Thus, our

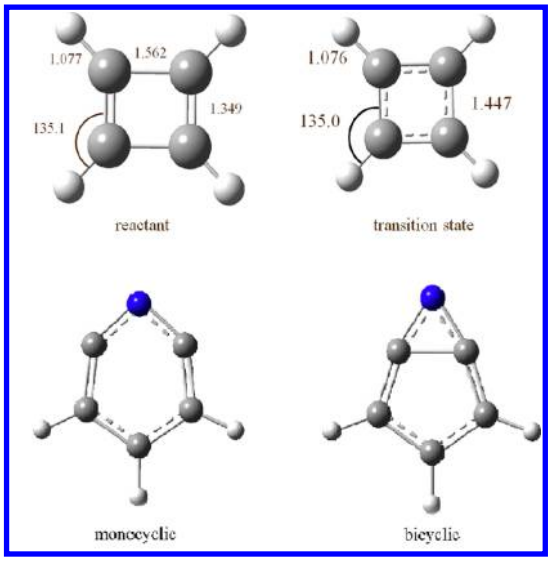

Figure 2. Structures of the reactant and the transition state of cyclobutadiene and the monocyclic and bicyclic forms of 2,6-pyridyne. The structural parameters of these species are taken from refs 57 and 60, respectively.

Table 7. ZPE-Corrected Energy Barriers (kcal/mol) for the Automerization of Cyclobutadiene Calculated with Different Methods at the Cartesian cc-pVTZ Basis Set[a]

methods	barriers (kcal/mol)
GVB(2)-BCPT2	18.59
CASCI-BCPT2/GVB(2)	11.81
CAS/A[b]	10.33 (6.92)
CASPT2	1.30
CAS-BCCC4[c]	6.21
MR-AQCC[d]	6.40
exptl.[e]	1.6−10.0

[a]The CASPT2, CAS-BCCC4, and MR-AQCC methods are calculated with the CASSCF(4,4) reference. [b]The CAS/A value based on the CASSCF orbitals is included in parentheses. [c]Ref 59. [d]Refs 57 (calculated with the spherical cc-pVTZ basis set). [e]Ref 58.

calculations on this reaction reveal that the accuracy of the CASCI-BCPT2/GVB method may decrease to some extent if the delocalization of GVB orbitals is significant.

D. The Energy Difference between the Monocyclic and Bicyclic Forms of 2,6-Pyridyne. The 2,6-isomers of didehydropyridine (pyridyne) are a very interesting class of compounds as they exhibit a wide range of multireference character, depending on the distance between the two radical centers. The geometries of the monocyclic and bicyclic forms of 2,6-pyridyne are taken from ref 60 (displayed in Figure 2), which are optimized with the Mk-MRCCSD (state-specific multireference coupled cluster singles and doubles) method developed by Mukherjee and co-workers at the cc-pCVTZ basis set. The Mk-MRCCSD and corresponding Mk-MRCCSD(T) (Mk-MRCCSD method with perturbative triples)[61] employ the restricted HF (RHF) determinant as the reference. Our GVB-BCPT2 and CASCI-BCPT2/GVB calculations are based on the GVB(4) orbitals, in which three geminals contain six π electrons in six π orbitals and the fourth geminal describes the σ bond between the radical centers. The calculated energy differences with various methods are listed in Table 8. The CCSD method incorrectly predicts the bicyclic structure to be

DOI: 10.1021/acs.jctc.5b00495
J. Chem. Theory Comput. 2015, 11, 4634−4643

Table 8. Relative Energies (kcal/mol) of the Monocyclic Form of 2,6-Pyridyne with Respect to the Bicyclic Form Calculated with Various Methods at the cc-pCVTZ Basis Set[a]

methods	energy difference (kcal/mol)
GVB(4)-BCPT2	3.4
CASCI-BCPT2/GVB(4)	4.9
CAS/A[b]	6.4 (5.4)
CCSD[c]	−3.6
CCSD(T)[c]	5.5
Mk-MRCCSD[c]	3.6
Mk-MRCCSD(T)[c]	8.8

[a]The Mk-MRCCSD and Mk-MRCCSD(T) calculations are based on a closed-shell HF reference. [b]The CAS/A value based on the CASSCF orbitals is included in parentheses. [c]Ref 61.

more stable by about 3.6 kcal/mol, while the other methods favor the monocyclic form to be the lowest-energy structure. Since the Mk-MRCCSD(T) method should be the most accurate method among these methods, the Mk-MRCCSD(T) value (8.8 kcal/mol) may be taken as the reference data. One can see that CASCI-BCPT2/GVB(4) predicts the energy difference to be 4.9 kcal/mol, being close to the CCSD(T) value (5.5 kcal/mol). The CAS/A energy differences based on the GVB and CASSCF orbitals are 6.4 and 5.4 kcal/mol, respectively. The analysis of the GVB orbitals shows that for these two structures the GVB orbitals are somewhat delocalized, but the delocalization extent of these GVB orbitals in both structures is quite similar.

IV. CONCLUSIONS

In this paper, we propose an alternative multireference perturbation theory based on a complete active space configuration interaction (CASCI) function or density matrix renormalized group (DMRG) function as the reference. The method may be considered as an approximation to the CAS/A approach with the same reference, in which the dynamical correlation is simplified with blocked correlated second order perturbation theory based on the generalized valence bond (GVB) reference. The present method, named CASCI-BCPT2/GVB or DMRG-BCPT2/GVB, is size consistent, and has a similar computational cost as the conventional MP2 method. We have applied the present method to investigate the bond-breaking potential energy surfaces in four molecules (H_2O, N_2, methane, and *n*-butane), the spectroscopic constants of six diatomic molecules, and the reaction barrier for the automerization of cyclobutadiene and the energy difference between the monocyclic and bicyclic forms of 2,6-pyridyne. Our test applications demonstrate that this method can provide comparable results as CASPT2 for multibond dissociation processes (when CASPT2 calculations are feasible) and much better results than GVB-BCPT2, especially when systems exhibit strong multireference character. Our calculations also show that the CASCI-BCPT2/GVB method would be a good approximation to the CAS/A method with the same GVB reference orbitals. However, when the GVB orbitals are quite delocalized in some systems, the performance of the CASCI-BCPT2/GVB method may become less satisfactory, since in such cases GVB orbitals may be not good approximations to the corresponding CASSCF orbitals. Furthermore, DMRG-BCPT2/GVB is applicable to strongly correlated systems with large active spaces, which are beyond the capability of CASPT2. DMRG-BCPT2/GVB has the potential to be a promising approach for describing the electronic structures of certain large systems, in which both the static correlation and dynamical correlation are very important.

It is worthwhile to mention how the perturbation approach described in this work can be further improved. In the present approach, the dynamical correlation is treated at the GVB-BCPT2 level. An obvious improvement is to treat the dynamical correlation up to the third-order block correlated perturbation theory. Other improvements on this method are also possible.

APPENDIX A: BLOCK-CORRELATED EXCITED OPERATORS REQUIRED IN THE CASCI-BCPT2/GVB METHOD

Three categories of block-correlated excitation operators (two-, three-, and four-block correlated operators) are needed in constructing the first-order wave function. The expressions of these block-correlated excitation operators are given for each category separately.

Two-block correlated operators:

$$\hat{T}_{2A} = \sum_{P}^{gem} \sum_{\lambda\in P}^{N_0-1} \sum_{r}^{vir} \hat{A}^{+}_{P_\lambda} \hat{A}^{-}_{P_0} r^{+} \tag{A1}$$

$$\hat{T}_{2B} = \sum_{P}^{gem} \sum_{\lambda\in P}^{N_0+1} \sum_{i}^{occ} \hat{A}^{+}_{P_\lambda} \hat{A}^{-}_{P_0} i^{-} \tag{A2}$$

$$\hat{T}_{2C} = \sum_{r}^{vir} \sum_{i}^{occ} r^{+} i^{-} \tag{A3}$$

Three-block correlated operators:

$$\hat{T}_{3A} = \sum_{P}^{gem} \sum_{\lambda\in P}^{N_0-2} \sum_{Q\neq P}^{gem} \sum_{\sigma\in Q}^{N_0+1} \sum_{r}^{vir} \hat{A}^{+}_{P_\lambda} \hat{A}^{-}_{P_0} \hat{A}^{+}_{Q_\sigma} \hat{A}^{-}_{Q_0} r^{+} \tag{A4}$$

$$\hat{T}_{3B} = \sum_{P}^{gem} \sum_{\lambda\in P}^{N_0-1} \sum_{Q\neq P}^{gem} \sum_{\sigma\in Q}^{N_0} \sum_{r}^{vir} \hat{A}^{+}_{P_\lambda} \hat{A}^{-}_{P_0} \hat{A}^{+}_{Q_\sigma} \hat{A}^{-}_{Q_0} r^{+} \tag{A5}$$

$$\hat{T}_{3C} = \sum_{P}^{gem} \sum_{\lambda\in P}^{N_0} \sum_{Q\neq P}^{gem} \sum_{\sigma\in Q}^{N_0+1} \sum_{i}^{occ} \hat{A}^{+}_{P_\lambda} \hat{A}^{-}_{P_0} \hat{A}^{+}_{Q_\sigma} \hat{A}^{-}_{Q_0} i^{-} \tag{A6}$$

$$\hat{T}_{3D} = \sum_{P}^{gem} \sum_{\lambda\in P}^{N_0-1} \sum_{Q\neq P}^{gem} \sum_{\sigma\in Q}^{N_0+2} \sum_{1}^{occ} \hat{A}^{+}_{P_\lambda} \hat{A}^{-}_{P_0} \hat{A}^{+}_{Q_\sigma} \hat{A}^{-}_{Q_0} i^{-} \tag{A7}$$

$$\hat{T}_{3E} = \sum_{P}^{gem} \sum_{\lambda\in P}^{N_0} \sum_{r}^{vir} \sum_{i}^{occ} \hat{A}^{+}_{P_\lambda} \hat{A}^{-}_{P_0} r^{+} i^{-} \tag{A8}$$

$$\hat{T}_{3F} = \frac{1}{2} \sum_{P}^{gem} \sum_{\lambda\in P}^{N_0-2} \sum_{r}^{vir} \sum_{s}^{vir} \hat{A}^{+}_{P_\lambda} \hat{A}^{-}_{P_0} r^{+} s^{+} \tag{A9}$$

$$\hat{T}_{3G} = \frac{1}{2} \sum_{P}^{gem} \sum_{\lambda\in P}^{N_0+2} \sum_{i}^{occ} \sum_{j}^{occ} \hat{A}^{+}_{P_\lambda} \hat{A}^{-}_{P_0} i^{-} j^{-} \tag{A10}$$

Four-block correlated operators:

DOI: 10.1021/acs.jctc.5b00495
J. Chem. Theory Comput. 2015, 11, 4634−4643

$$\hat{T}_{4A} = \frac{1}{2}\sum_{P}^{\text{gem}}\sum_{\lambda\in P}^{N_0-1}\sum_{Q\neq P}^{\text{gem}}\sum_{\sigma\in Q}^{N_0-1}\sum_{R\neq P,Q}^{\text{gem}}\sum_{\omega\in R}^{N_0+1}\sum_{r}^{\text{vir}}\hat{A}_{P_\lambda}^{+}\hat{A}_{P_0}^{-}\hat{A}_{Q_\sigma}^{+}\hat{A}_{Q_0}^{-}\hat{A}_{R_\omega}^{+}\hat{A}_{R_0}^{-}r^{+} \tag{A11}$$

$$\hat{T}_{4B} = \frac{1}{2}\sum_{P}^{\text{gem}}\sum_{\lambda\in P}^{N_0-1}\sum_{Q\neq P}^{\text{gem}}\sum_{\sigma\in Q}^{N_0+1}\sum_{R\neq P,Q}^{\text{gem}}\sum_{\omega\in R}^{N_0+1}\sum_{i}^{\text{occ}}\hat{A}_{P_\lambda}^{+}\hat{A}_{P_0}^{-}\hat{A}_{Q_\sigma}^{+}\hat{A}_{Q_0}^{-}\hat{A}_{R_\omega}^{+}\hat{A}_{R_0}^{-}i^{-} \tag{A12}$$

$$\hat{T}_{4C} = \frac{1}{4}\sum_{P}^{\text{gem}}\sum_{\lambda\in P}^{N_0-1}\sum_{Q\neq P}^{\text{gem}}\sum_{\sigma\in Q}^{N_0-1}\sum_{r}^{\text{vir}}\sum_{s}^{\text{vir}}\hat{A}_{P_\lambda}^{+}\hat{A}_{P_0}^{-}\hat{A}_{Q_\sigma}^{+}\hat{A}_{Q_0}^{-}r^{+}s^{+} \tag{A13}$$

$$\hat{T}_{4D} = \sum_{P}^{\text{gem}}\sum_{\lambda\in P}^{N_0-1}\sum_{Q\neq P}^{\text{gem}}\sum_{\sigma\in Q}^{N_0+1}\sum_{r}^{\text{vir}}\sum_{i}^{\text{occ}}\hat{A}_{P_\lambda}^{+}\hat{A}_{P_0}^{-}\hat{A}_{Q_\sigma}^{+}\hat{A}_{Q_0}^{-}r^{+}i^{-} \tag{A14}$$

$$\hat{T}_{4E} = \frac{1}{4}\sum_{P}^{\text{gem}}\sum_{\lambda\in P}^{N_0+1}\sum_{Q\neq P}^{\text{gem}}\sum_{\sigma\in Q}^{N_0+1}\sum_{i}^{\text{occ}}\sum_{j}^{\text{occ}}\hat{A}_{P_\lambda}^{+}\hat{A}_{P_0}^{-}\hat{A}_{Q_\sigma}^{+}\hat{A}_{Q_0}^{-}i^{-}j^{-} \tag{A15}$$

$$\hat{T}_{4F} = \frac{1}{2}\sum_{P}^{\text{gem}}\sum_{\lambda\in P}^{N_0-1}\sum_{r}^{\text{vir}}\sum_{s}^{\text{vir}}\sum_{i}^{\text{occ}}\hat{A}_{P_\lambda}^{+}\hat{A}_{P_0}^{-}r^{+}s^{+}i^{-} \tag{A16}$$

$$\hat{T}_{4G} = \frac{1}{2}\sum_{P}^{\text{gem}}\sum_{\lambda\in P}^{N_0+1}\sum_{r}^{\text{vir}}\sum_{i}^{\text{occ}}\sum_{j}^{\text{occ}}\hat{A}_{P_\lambda}^{+}\hat{A}_{P_0}^{-}r^{+}i^{-}j^{-} \tag{A17}$$

$$\hat{T}_{4H} = \frac{1}{4}\sum_{r}^{\text{vir}}\sum_{s}^{\text{vir}}\sum_{i}^{\text{occ}}\sum_{j}^{\text{occ}}r^{+}s^{+}i^{-}j^{-} \tag{A18}$$

In the formulations above, N_0 represents the number of electrons in the ground state of each geminal block. In the GVB reference, N_0 is always equal to 2.

In CASCI-BCPT2/GVB, the orbital indices in $\hat{T}_u^{\text{GVB}}$ also include the open-shell orbitals, in addition to closed-shell and virtual orbitals. However, the block correlated operators only involving active blocks (geminals or open-shell orbitals) should be excluded. While in CAS/A, since the active block consists of all geminals and open-shell orbitals, only $\hat{T}_{2A}$, $\hat{T}_{2B}$, $\hat{T}_{2C}$, $\hat{T}_{3E}$, $\hat{T}_{3F}$, $\hat{T}_{3G}$, $\hat{T}_{4F}$, $\hat{T}_{4G}$, and $\hat{T}_{4H}$ operators are needed. For CAS/A, N_0 is just the number of active electrons.

APPENDIX B: THE COMPUTATION OF THE MATRIX ELEMENTS $\langle\Psi_0^{\text{GVB}}|(\hat{H}-\hat{H}_0^{\text{GVB}})|\Psi_U^{\text{GVB}}\rangle$

In the following, we will give some details on how to compute the matrix elements, $\langle\Psi_0^{\text{GVB}}|(\hat{H}-\hat{H}_0^{\text{GVB}})|\Psi_u^{\text{GVB}}\rangle$, involved in eq 13.

Since both $|\Psi_0^{\text{GVB}}\rangle$ and $\{|\Psi_u^{\text{GVB}}\rangle\}$ are the eigenfunctions of $\hat{H}_0^{\text{GVB}}$, we have

$$\langle\Psi_0^{\text{GVB}}|\hat{H}_0^{\text{GVB}}|\Psi_u^{\text{GVB}}\rangle = 0 \tag{B1}$$

Then,

$$\langle\Psi_0^{\text{GVB}}|(\hat{H}-\hat{H}_0^{\text{GVB}})|\Psi_u^{\text{GVB}}\rangle = \langle\Psi_0^{\text{GVB}}|\hat{H}|\Psi_u^{\text{GVB}}\rangle \tag{B2}$$

Using the second-quantized form of the electronic Hamiltonian, we have developed a computer program to generate the expressions of $\langle\Psi_0^{\text{GVB}}|\hat{H}|\Psi_u^{\text{GVB}}\rangle$ for all excited configurations. For instance, some matrix elements can be computed as listed below:

$$\hat{T}_{4B}\Psi_0^{\text{GVB}} = \frac{1}{2}\sum_{P}^{\text{gem}}\sum_{\lambda\in P}^{N_0-1}\sum_{Q\neq P}^{\text{gem}}\sum_{\sigma\in Q}^{N_0+1}\sum_{R\neq P,Q}^{\text{gem}}\sum_{\omega\in R}^{N_0+1}\sum_{i}^{\text{occ}}\hat{A}_{P_\lambda}^{+}\hat{A}_{P_0}^{-}\hat{A}_{Q_\sigma}^{+}\times\hat{A}_{Q_0}^{-}\hat{A}_{R_\omega}^{+}\hat{A}_{R_0}^{-}i^{-}\Psi_0^{\text{GVB}} = \frac{1}{2}\sum_{u}\Psi_u^{\text{GVB}} \tag{B3}$$

$$\Psi_u^{\text{GVB}} = \hat{A}_{P_\lambda}^{+}\hat{A}_{P_0}^{-}\hat{A}_{Q_\sigma}^{+}\hat{A}_{Q_0}^{-}\hat{A}_{R_\omega}^{+}\hat{A}_{R_0}^{-}i^{-}\Psi_0^{(0)} \tag{B4}$$

$$\langle\Psi_0^{\text{GVB}}|\hat{H}|\Psi_u^{\text{GVB}}\rangle = \sum_{w\in P}\sum_{x\in Q}\sum_{y\in R}\langle iw||xy\rangle\times\langle P_0|w^{+}|P_\lambda\rangle\times\langle Q_0|x^{-}|Q_\sigma\rangle\times\langle R_0|y^{-}|R_\omega\rangle \tag{B5}$$

AUTHOR INFORMATION

Corresponding Author

*E-mail: shuhua@nju.edu.cn.

Notes

The authors declare no competing financial interest.

ACKNOWLEDGMENTS

This work was supported by the National Natural Science Foundation of China (Grant No. 21333004) and the National Basic Research Program (Grant No. 2011CB808501). All calculations in this work have been done on the IBM Blade cluster system in the High Performance Computing Center of Nanjing University.

REFERENCES

(1) Wolinski, K.; Sellers, H. L.; Pulay, P. *Chem. Phys. Lett.* **1987**, *140*, 225−231.
(2) Wolinski, K.; Pulay, P. *J. Chem. Phys.* **1989**, *90*, 3647−3659.
(3) Andersson, K.; Malmqvist, P.; Roos, B. O.; Sadlej, A. J.; Wolinski, K. *J. Phys. Chem.* **1990**, *94*, 5483−5488.
(4) Andersson, K.; Malmqvist, P.; Roos, B. O. *J. Chem. Phys.* **1992**, *96*, 1218−1226.
(5) Dyall, K. G. *J. Chem. Phys.* **1995**, *102*, 4909−4918.
(6) Mahapatra, U. S.; Datta, B.; Mukherjee, D. *J. Phys. Chem. A* **1999**, *103*, 1822−1830.
(7) Mao, S.; Cheng, L.; Liu, W.; Mukherjee, D. *J. Chem. Phys.* **2012**, *136*, 024105.
(8) Mao, S.; Cheng, L.; Liu, W.; Mukherjee, D. *J. Chem. Phys.* **2012**, *136*, 024106.
(9) Lyakh, D. I.; Musial, M.; Lotrich, V. F.; Bartlett, R. J. *Chem. Rev.* **2012**, *112*, 182−243.
(10) Jeziorski, B.; Monkhorst, H. J. *Phys. Rev. A: At., Mol., Opt. Phys.* **1981**, *24*, 1668−1681.
(11) Jeziorski, B.; Paldus, J. *J. Chem. Phys.* **1988**, *88*, 5673−5687.
(12) Paldus, J.; Piecuch, P.; Pylypow, L.; Jeziorski, B. *Phys. Rev. A: At., Mol., Opt. Phys.* **1993**, *47*, 2738−2782.
(13) Kutzelnigg, W. *J. Chem. Phys.* **1982**, *77*, 3081−3097.
(14) Mahapatra, U. S.; Datta, B.; Mukherjee, D. *J. Chem. Phys.* **1999**, *110*, 6171−6188.
(15) Evangelista, F. A.; Allen, W. D.; Schaefer, H. F., III *J. Chem. Phys.* **2007**, *127*, 024102.
(16) Fang, T.; Li, S. *J. Chem. Phys.* **2007**, *127*, 204108.
(17) Fang, T.; Shen, J.; Li, S. *J. Chem. Phys.* **2008**, *128*, 224107.
(18) Das, S.; Pathak, S.; Datta, D.; Mukherjee, D. *J. Chem. Phys.* **2012**, *136*, 164104;(Erratum) **2012**, *137*, 069901.
(19) Hanauer, M.; Kohn, A. *J. Chem. Phys.* **2012**, *136*, 204107.
(20) Chen, Z.; Hoffmann, M. R. *J. Chem. Phys.* **2012**, *137*, 014108.
(21) Demel, O.; Kedzuch, S.; Noga, J.; Pittner, J. *Mol. Phys.* **2013**, *111*, 2477−2488.

DOI: 10.1021/acs.jctc.5b00495
J. Chem. Theory Comput. 2015, 11, 4634−4643

(22) Kurashige, Y.; Yanai, T. *J. Chem. Phys.* **2013**, *135*, 094104.
(23) Sharma, S.; Chan, G. K.-L. *J. Chem. Phys.* **2014**, *141*, 111101.
(24) Bobrowicz, F. W.; Goddard, W. A., III. *Methods of Electronic Structure Theory*; Plenum, New York, 1977; p 79.
(25) Xu, E.; Li, S. *J. Chem. Phys.* **2013**, *139*, 174111.
(26) White, S. R. *Phys. Rev. Lett.* **1992**, *69*, 2863−2866.
(27) Schollwöck, U. *Rev. Mod. Phys.* **2005**, *77*, 259−315.
(28) Chan, G. K.-L.; Sharma, S. *Annu. Rev. Phys. Chem.* **2011**, *62*, 465−481.
(29) Kozlowski, P. M.; Davidson, E. R. *J. Chem. Phys.* **1994**, *100*, 3672−3682.
(30) Schmidt, M. W.; Baldridge, K. K.; Boatz, J. A.; Elbert, S. T.; Gordon, M. S.; Jensen, J. H.; Koseki, S.; Matsunaga, N.; Nguyen, K. A.; Su, S. J.; Windus, T. L.; Dupuis, M.; Montgomery, J. A. *J. Comput. Chem.* **1993**, *14*, 1347−1363.
(31) Chan, G. K.-L.; Head-Gordon, M. *J. Chem. Phys.* **2002**, *116*, 4462−4476.
(32) Chan, G. K.-L. *J. Chem. Phys.* **2004**, *120*, 3172−3178.
(33) Ghosh, D.; Hachmann, J.; Yanai, T.; Chan, G. K.-L. *J. Chem. Phys.* **2008**, *128*, 144117.
(34) Sharma, S.; Chan, G. K.-L. *J. Chem. Phys.* **2012**, *136*, 124121.
(35) Werner, H.-J. *Mol. Phys.* **1996**, *89*, 645−661.
(36) Celani, P.; Werner, H.-J. *J. Chem. Phys.* **2000**, *112*, 5546−5557.
(37) Ghigo, G.; Roos, B. O.; Malmqvist, P. A. *Chem. Phys. Lett.* **2004**, *396*, 142−149.
(38) Werner, H.-J.; Knowles, P. J.; Knizia, G.; Manby, F. R.; Schütz, M.; Celani, P.; Korona, T.; Lindh, R.; Mitrushenkov, A.; Rauhut, G.; Shamasundar, K. R.; Adler, T. B.; Amos, R. D.; Bernhardsson, A.; Berning, A.; Cooper, D. L.; Deegan, M. J. O.; Dobbyn, A. J.; Eckert, F.; Goll, E.; Hampel, C.; Hesselmann, A.; Hetzer, G.; Hrenar, T.; Jansen, G.; Köppl, C.; Liu, Y.; Lloyd, A. W.; Mata, R. A.; May, A. J.; McNicholas, S. J.; Meyer, W.; Mura, M. E.; Nicklass, A.; O'Neill, D. P.; Palmieri, P.; Peng, D.; Pflüger, K.; Pitzer, R.; Reiher, M.; Shiozaki, T.; Stoll, H.; Stone, A. J.; Tarroni, R.; Thorsteinsson, T.; Wang, M. *MOLPRO*, version 2012.1; Institut für Theoretische Chemie, Universität Stuttgart: Stuttgart, Germany, 2012 (see http://www.molpro.net).
(39) Čížek, J. *J. Chem. Phys.* **1966**, *45*, 4256−4266.
(40) Paldus, J.; Čížek, J.; Shavitt, I. *Phys. Rev. A: At., Mol., Opt. Phys.* **1972**, *5*, 50−67.
(41) Bartlett, R. J.; Purvis, G. D. *Int. J. Quantum Chem.* **1978**, *14*, 561−581; *Phys. Scr.* **1980**, *21*, 251−255.
(42) Purvis, G. D.; Bartlett, R. J. *J. Chem. Phys.* **1982**, *76*, 1910−1918.
(43) Raghavachari, K.; Trucks, G. W.; Pople, J. A.; Head-Gordon, M. *Chem. Phys. Lett.* **1989**, *157*, 479−483.
(44) Mallard, W. G. *NIST Chemistry WebBook* (accessed June, 2005). http://webbook.nist.gov/chemistry.
(45) Merer, A. J. *Annu. Rev. Phys. Chem.* **1989**, *40*, 407−438.
(46) Dunn, T. M.; Hanson, K. L.; Rubinson, R. A. *Can. J. Phys.* **1970**, *48*, 1657.
(47) Douglas, A. E.; Veillette, P. M. *J. Chem. Phys.* **1980**, *72*, 5378−5380.
(48) Simard, B.; Masoni, C.; Hackett, P. A. *J. Mol. Spectrosc.* **1989**, *136*, 44−55.
(49) Bondybey, V. E.; English, J. H. *Chem. Phys. Lett.* **1983**, *94*, 443−447.
(50) Casey, S. M.; Leopold, D. G. *J. Phys. Chem.* **1993**, *97*, 816−830.
(51) Hilpert, K.; Ruthard, K. *Ber. Bunsenges. Phys. Chem.* **1987**, *91*, 724−731.
(52) Su, C. X.; Hales, D. A.; Armentrout, P. B. *Chem. Phys. Lett.* **1993**, *201*, 199−204.
(53) Simard, B.; Lebeault-Dorget, M. A.; Marijnissen, A.; Ter Meulen, J. J. *J. Chem. Phys.* **1998**, *108*, 9668−9674.
(54) Roos, B. O. *Acc. Chem. Res.* **1999**, *32*, 137−144.
(55) Kurashige, Y.; Yanai, T. *J. Chem. Phys.* **2011**, *135*, 094104.
(56) Müller, T. *J. Phys. Chem. A* **2009**, *113*, 12729−12740.
(57) Eckert-Maksić, M.; Vazdar, M.; Barbatti, M.; Lischka, H.; Maksić, Z. B. *J. Chem. Phys.* **2006**, *125*, 064310.
(58) Whitman, D. W.; Carpenter, B. K. *J. Am. Chem. Soc.* **1982**, *104*, 6473−6474. Carpenter, B. K. *J. Am. Chem. Soc.* **1983**, *105*, 1700−1701.
(59) Shen, J.; Fang, T.; Li, S.; Jiang, J. *J. Phys. Chem. A* **2008**, *112*, 12518−12525.
(60) Prochnow, E.; Evangelista, F. A.; Schaefer, H. F.; Allen, W. D.; Gauss, J. *J. Chem. Phys.* **2009**, *131*, 064109.
(61) Evangelista, F. A.; Prochnow, E.; Gauss, J.; Schaefer, H. F. *J. Chem. Phys.* **2010**, *132*, 074107.

NOTE ADDED AFTER ASAP PUBLICATION

This article was posted ASAP on September 15, 2015. In Table 2, the DMRG data for N_2 for the distance Re = 3.6 and 4.5 in cc-PVTZ basis has been corrected. The corrected version was published on September 25, 2015.

DOI: 10.1021/acs.jctc.5b00495
J. Chem. Theory Comput. 2015, 11, 4634−4643